REVISITING (ANTI)AROMATICITY AND CHEMICAL BOND IN PLANAR B_XN_X CLUSTERS (X = 2 – 11)

Lily Arrué[1] and Ricardo Pino-Rios[2]

[1]Universidad Autonoma de Chile - Campus Providencia
[2]Universidad de Santiago de Chile

April 29, 2020

Abstract

The aromaticity of boron-nitrogen clusters has been revisited through a systematic analysis using magnetic criteria. The results obtained through Ring Current Strength (RCS) measurements indicate that B^2N_2 has a strongly antiaromatic character, even the bond pattern analysis reveals that this system is doubly antiaromatic presenting two σ- and two π-orbitals of 4c-2e, according to the Adaptive Natural Density Partitioning bond pattern analysis (AdNDP) and z-component of the dissected Nucleus Independent Chemical Shift ($NICS_{zz}$) isolines. B_4N_4 and B_6N_6 are marginally antiaromatic according to RCS and the bond pattern suggest four and six 8c-2e and 12c-2e delocalized π-orbitals respectively. B_3N_3 and B_5N_5 are slightly aromatic, with a bond pattern of three and five 6c-2e and 10c-2e π-orbitals respectively. All rest of the systems (x = 7 – 11) are non-aromatic. The results show some discrepancies with results based on the classical nucleus independent chemical shift, which can be attributed to tensor in-plane and core electron contributions. Finally, presented results reveal the need to be careful with the interpretations given by this index, so it will be necessary the use of 1D, 2D or 3D derived methodologies for a complete and correct analysis of (anti)aromaticity.

INTRODUCTION

Mixed boron-nitrogen (BN) materials have been subject of both experimental and theoretical studies in order to understand their properties[1], such as their thermal stability for example, hexagonal boron nitride (h-BN) are analogous to graphene and has been used as thermally stable engineering ceramic and most recently in optoelectronic devices[2]. Additionally, BN clusters are interesting due to their participation in formation of thin solid films of β-BN, that possess the particularity of scratching diamond[3]. Recently, the application of atomic clusters as assembly blocks for the design of new materials has grown in interest and the term "Cluster Assembled Materials" (CAM) has been coined[4], so knowing the structures and electronic properties of these clusters is of great importance[5]. B_xN_y clusters have been characterized through the interaction between pulsed laser evaporation followed by matrix infrared spectroscopy and theoretical predictions[6,7]. On the other hand, B_xN_x clusters offer three-dimensional structures that are similar to fullerene. $B_{12}N_{12}$, $B_{76}N_{76}$, $B_{208}N_{208}$, among others, these have been obtained through intense irradiation of boron nitride samples[8,9]. Furthermore, small clusters offer planar structures that resemble carbon clusters[10].

Some years ago, Matxain *et al* .[11] carried out an exhaustive analysis of the potential energy surface (PES) of B_xN_x clusters (x = 2 – 15) in singlet state through Quantum Monte-Carlo calculations in order to know the geometries of these clusters, obtaining as global minima planar structures for x = 2 – 11 and three-dimensional for x = 12 - 15. Additionally, authors concluded that planar structures with 2, 3, 5, 7 BN moieties are π-aromatic, structures with 4, 6 moieties are antiaromatic and 8 – 11 BN moieties are non-aromatic according to their Nucleus Independent Chemical Shift (NICS) calculations. Results for B_2N_2 are counter intuitive according to traditional electron counting rules such as Hückel's rule[12], which states that cyclic systems with 4n+2 (4n) electrons have an aromatic (antiaromatic) character. Along with this, the

difference in electronegativities between the B and N atoms leads to a very different electronic distribution than typical organic aromatic systems, leading to a reduction in aromaticity. This characteristic has been studied in various systems such as cyclotriphosphazenes, metallabenzenes, among others[13-16].

The concept of aromaticity[17], despite not being an experimental observable, has been of great utility to rationalize stability, electronic structure and chemical bond among other properties in organic and inorganic chemistry[18]. There are several criteria to rationalize aromaticity, such as the geometric[19], electronic delocalization[20] and the magnetic criteria[21], being the latter the latter being very popular in recent years. In 1996, Schleyer *et al* . proposed the Nucleus independent chemical shift (NICS)[22], defined as the negative of the isotropic magnetic shielding evaluated at the centre of the ring of an (anti)aromatic system. This index quickly became popular due to its ease calculation in many standard quantum chemical software. However, its indiscriminate use has been criticized by several authors, indicating that the validity of the NICS is limited due to spurious contributions from the in-plane tensor components which are not related with aromaticity[23-31].

To avoid these problems, different ways to analyse NICS have been suggested. For instance: to compute the property 1.0 angstrom (Å) above the molecular plane NICS(1)[32], and to evaluate the out-of-plane component of the NICS tensor, the so called $NICS_{zz}$ which has been proven to be particularly sensitive to π-electron delocalization[33,34]. Other strategies proposed are related to the analysis of NICS in the axis perpendicular to the molecular plane. Stanger *et al* .[35] and Solá *et al.* [36], independently, proposed NICS scans and more recently Torres-Vega*et al* .[13] proposed the FiPC-NICS strategy which allows to obtain characteristic profiles for aromatic, antiaromatic, and non-aromatic molecules. Another more sophisticated approaches are related to dissected NICS approaches, bi-dimensional maps, three-dimensional grids and quantification related to its topology[37-41].

In this article the aromaticity of $B_xN_x$clusters (x = 2 – 11) has been revisited by means of magnetic criteria of aromaticity, and chemical bond has been analysed through Adaptative Natural Density Partitioning (AdNDP) method[42,43]. A complete analysis considering different NICS-based strategies proposed in literature were carried out. Additionally, ring current strengths (RCS) were computed measuring the flow of ring current passing through interatomic surfaces according to quantum theory of atoms in molecules (QTAIM) proposed by Bader[44-47].

COMPUTATIONAL METHODS

Planar B_xN_x (x = 2 – 11) clusters were optimized at the PBE0[48]/def2-TZVP[49]level of theory using Gaussian 09 computational package[50]. For the fully optimized molecules, vibrational frequency calculations were performed at the same level to ensure that we obtained a true minimum on the potential energy surface. $NICS_{zz}$ values were computed employing the Gauge-Including Atomic Orbital (GIAO) in gas phase at the above-mentioned level. Ring current strength (RCS) calculations were done using AIMAll[51] software. Chemical bond was analysed through Adaptative Natural Density Partitioning (AdNDP), this method is a generalization of NBO method. AdNDP recovers Lewis bonding (1c-2e lone pairs, 2c-2e two electron bonds), additionally, localized bonds associated with (anti)aromaticity. $NICS_{zz}$ scans, FiPC and $NICS_{zz}$ isosurfaces and AdNDP orbitals were obtained using our own routines and Multiwfn software[52]. Visualization of $NICS_{zz}$isosurfaces and $NICS_{zz}$ isolines have been plotted using Chemcraft and VisIt 2.13.0 respectively[53,54].

RESULTS AND DISCUSSION

Quantifying aromaticity according to ring current strength (RCS) and $NICS_{zz}$ based descriptors

Systems studied in this work are $B_xN_x$clusters (x = 2 – 11) depicted in Fig. S1 in the supporting information. This section is aimed to the quantification of the (anti)aromatic character of the mentioned clusters. For this purpose, ring current strengths (RCS) were computed and compared with different quantification strategies based on $NICS_{zz}$. RCS values were obtained by numerical integration of the current flow through interatomic surfaces by means of quantum theory of atoms in molecules (QTAIM) proposed by Bader. RCS values have

been widely used in aromaticity studies and are known to be a reliable indicator of the (anti)aromatic character of both organic and inorganic systems. According to table 1, B_2N_2, present a strong antiaromatic character with a RCS value of -13.0 nA.T^{-1} in clear disagreement with Matxain *et al* . results but consistent with electron counting rules.

B_4N_4 and B_6N_6, present low negative values (-2.7 and -1.5 nA.T^{-1} respectively) revealing weak antiaromaticity. On the other hand, borazine-like B_3N_3 present a RCS value of 3.8 nA.T^{-1}, in agreement with recent reported results[55], whereas B_5N_5 have a RCS value 2.2 nA.T^{-1} revealing its weak aromatic character. The rest of the systems (x = 7 – 11) show values close to zero, therefore, they are non-aromatic. Additionally, $NICS_{zz}$ was measurement at 0.0 Å, 1.0 Å, 2.0 Å and FiPC (Free in plane component, where the in-plane contributions are zero) can be seen in Fig. 1, these values correlate quite well with the RCS, however it is necessary to be very cautious with the interpretation. As an example, let us take the $NICS_{zz}(1)$ value of B_5N_5, which is -0.44 ppm, this result can be interpreted as non-aromatic and not (weak) aromatic, as indicated by its RCS value. The same behaviour is observed for the $NICS_{zz}(2)$ of B_4N_4 (0.32 ppm) which could be interpreted as non-aromatic, however the RCS values showed that this system is (weak) antiaromatic.

Table 1. RCS (in nA.T^{-1}) values and $NICS_{zz}$ (in ppm?) computations for the B_xN_x (x = 2 – 11) planar clusters. RCS positive (negative values denote aromaticity (antiaromaticity), values close to zero, nor aromatic character. Negative (Positive) values of NICSzz descriptors states an aromatic (Antiaromatica) character, whereas values close to zero are for non-aromatic compounds.

B_xN_x	RCS	$NICS_{zz}(0)$	$NICS_{zz}(1)$	$NICS_{zz}(2)$	FiPC-NICS
B_2N_2	-13.0	16.88	42.08	3.50	16.01
B_3N_3	3.8	-7.36	-6.05	-1.88	-6.39
B_4N_4	-2.7	19.90	10.17	0.32	7.48
B_5N_5	2.2	4.68	-0.44	-1.29	-2.14
B_6N_6	-1.5	11.36	6.92	0.47	3.72
B_7N_7	-0.9	4.49	2.20	-0.26	-0.35
B_8N_8	-0.6	6.09	4.34	0.50	1.49
B_9N_9	-0.3	3.52	2.47	0.21	0.33
$B_{10}N_{10}$	-0.3	3.65	2.89	0.46	0.72
$B_{11}N_{11}$	0.1	2.63	2.11	0.35	0.37

When we compare it with NICS based descriptors at 0, 1 and 2 Å above the plane, we can see that the first two do not correlate with RCS values (See Fig. S2 in SI), this behaviour can be attributed to contributions in the NICS plane and also to contributions from the core electrons of electronegative atoms. It is for this reason that NICS(2) presents a good correlation with the RCS values because the interference at this height is expected to be close to zero. These results confirm that one must be careful in the assignment of (anti)aromaticity using this index. The following sections are intended to perform an exhaustive qualitative analysis of the (anti)aromaticity of these clusters using different strategies proposed in the literature.

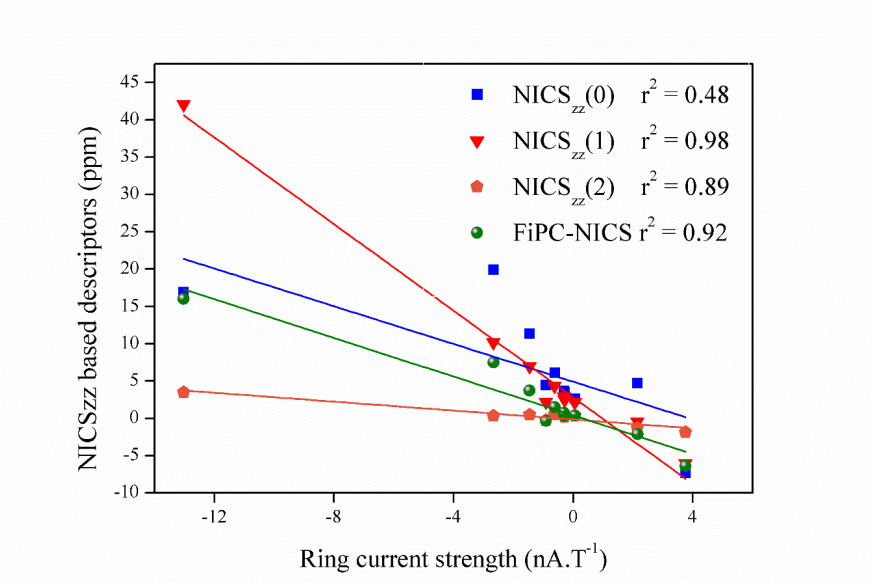

Fig. 1. Comparisons between ring current strength (RCS) values and $NICS_{zz}$based descriptors performed at PBE0/def2-TZVP.

Evaluation of NICS changes along the main molecular axis

In this part, discussion starts analysing FiPC-NICS strategy, proposed as a simplification of Stanger scans proposal. This strategy assumes of that in-plane components are more sensitive to local induced fields arising from the core and localized (lone pairs and bonding) electrons. Local magnetic fields should be of short-range which means that they should decay in small spatial intervals. In contrast, the out-of-plane component is expected to highlight the induced magnetic field, as is the case of aromatic and antiaromatic system. According to this strategy, one can classify an aromatic (antiaromatic) system if it has a convex (concave) slope, while a non-aromatic system behaves linearly. Fig. 2 shows that B_3N_3 and B_5N_5 can be classified as aromatic while B_2N_2, B_4N_4 and B_6N_6 are antiaromatic in agreement with our RCS values. The rest of the systems (x = 7 - 11) present a linear behaviour revealing its non-aromatic character. Additionally, is important to identify the distance where the in-plane components of NICS becomes zero. This distance for B_2N_2 and B_3N_3 are 1.7 and 1.1 Å respectively. The difference between distances are attributed to the local contributions of the core electrons, being greater for B_2N_2 due to the electronegativity of nitrogen atoms and a smaller ring size. For the rest of the systems, the distance increases systematically from 1.2 Å for the B_4N_4 to 2.7 Å for the $B_{11}N_{11}$. However, the increase in ring size and the non-aromatic character of the clusters makes contributions greater than 1.2 Å negligible (less than 1.0 ppm).

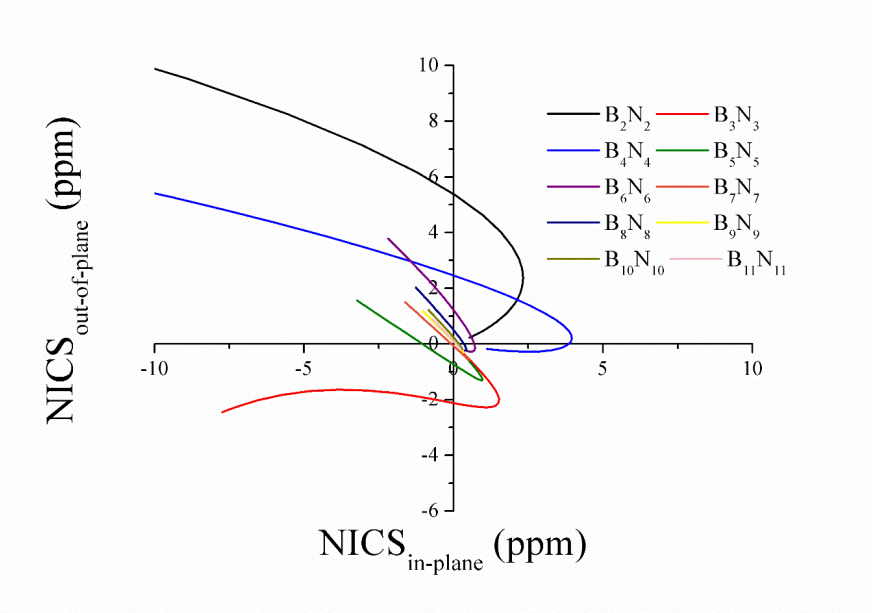

Fig. 2. Plots of the $NICS_{in\text{-}plane}$ vs. $NICS_{out\text{-}of\text{-}plane}$ for BxNx clusters (x = 3 – 11).

Complementary, $NICS_{zz}$-scans are showed in Fig. 3, measurements were carried out at center of the ring and above up to 5 Å. Through these plots it is possible to see the long-range effects characteristic of (anti)aromatic systems. B_3N_3 is the only system which presents long-range negative values characteristic for aromatic systems.

For B_5N_5, no long-range effects are observed, in disagreement with the RCS values which classify it as weakly aromatic, but in agreement with the $NICS_{zz}$values. Recently, Cina pointed out that when NICS values moves from negative to positive regions are good candidates for NICS failures which is the case of this cluster[56]. Additionally, this system presents two minimum values of -7.4 ppm and -6.8 ppm at 0.0 and 1.4 Å respectively, this may be due to local contributions from core electrons, these local contributions have been studied and are important in similar systems such as borazine[57].

On the other hand, B_2N_2, B_4N_4 and B_6N_6 present positive long-range values which is consistent with their antiaromatic character, while aromatic (According RCS calculations) B_5N_5 and B_7N_7 present small short-range. The rest systems have very low values due to the contributions of the core electrons.

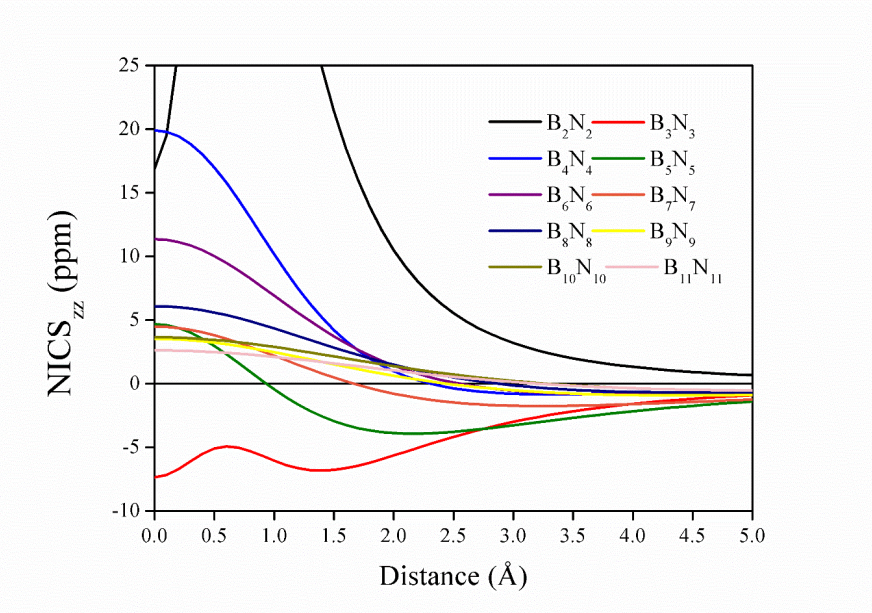

Fig. 3. $NICS_{zz}$ (ppm) vs. distance (in Angstrom) at PBE0/def2-TZVP level

Evaluation of $NICS_{zz}$ Isosurfaces

A three-dimensional analysis to assess the anisotropic effects of $NICS_{zz}$ was carried out, providing more insights regarding the (anti)aromaticity of the B_xN_x clusters. $NICS_{zz}$isosurfaces are depicted in Fig. 4. The presence of long-range diatropic regions inside the rings are indicative of their aromatic character. This can be observed in B_3N_3 where diatropic zones are located at the center and, additionally, located in nitrogen atoms due to the contributions of core electrons. The opposite effect can be seen B_2N_2, B_4N_4 and B_6N_6, where strong paratropic long-range zones are located at the center of these rings, denoting their antiaromatic character. Along with this, the diatropic zones located in the nitrogen atoms are also observed.

In B_5N_5, diatropic zones in nitrogen atoms and above the molecular ring are observed, however it is possible to see paratropic values at the centre of the ring, this characteristic pattern has been observed in non-aromatic organic systems including cyclopropane and cyclohexane[58]. The rest of the systems present diatropic regions located in the nitrogen atoms and short range paratropic zones in the center of the ring, characteristic of its non-aromatic nature.

Hosted file

`image4.emf` available at https://authorea.com/users/316479/articles/446619-revisiting-anti-aromaticity-and-chemical-bond-in-planar-bxnx-clusters-x-2-11

Fig. 4. $NICS_{zz}$ isosurfaces for B_xN_x clusters (x = 3 – 11) at +/- 4 ppm isovalue. Blue color represents negative (diatropic) values and red color represent positive (paratropic) values.

In order to gain more insights about the (anti)aromaticity patterns in "problematic" B_2N_2 and B_5N_5, dissected $NICS_{zz}$isolines have been obtained which allows us to observe in detail the contributions of the core, σ and π electrons, results are shown in Fig. 5. In the case of B_2N_2, core electron contributions to $NICS_{zz}$ present small diatropic short-range values. Surprisingly, σ-electron contributions present unexpected paratropic long-range pattern which resembles antiaromatic compounds, whereas π-electron contributions shows to an antiaromatic pattern, concluding that this cluster is doubly antiaromatic.

Hosted file

image5.emf available at https://authorea.com/users/316479/articles/446619-revisiting-anti-aromaticity-and-chemical-bond-in-planar-bxnx-clusters-x-2-11

Fig. 5. Isolines of dissected $NICS_{zz}$ for B_2N_2 and B_5N_5clusters.

Isolines of $B_5N_5NICS_{core,zz}$, have not negligible long range diatropic values according to the isosurface of $NICS_{zz}$ previously shown, where the diatropicity is located nitrogen atoms. Contributions of σ-electrons present short-range paratropic values in the center of molecular plane as seen in the $NICS_{zz}$ isosurface of B_5N_5. The contributions of π-electrons show long-range pattern that allows us to say that this cluster is weakly π-aromatic in agreement with RCS values.

Analyzing bonding pattern of B_xN_x clusters via Adaptative Natural Density Partitioning (AdNDP)

For a more detailed analysis regarding the aromaticity and chemical bond in B_xN_x clusters, AdNDP was performed, representative cases (antiaromatic, aromatic and non-aromatic) are shown in Fig. 6 and Fig. 7, the remaining systems can be seen in the supporting information.

The bonding pattern for B_2N_2 (Fig. 6) starts with four 2c-2e B-N σ bonds, it is necessary to note that the bonds are polarized towards N atoms mainly due to their high electronegativities regarding B atoms. In addition, two σ- and two π- delocalized 4c-2e bonds fullfilling electron counting rules which confirms their doubly aromatic character.

Hosted file

image6.emf available at https://authorea.com/users/316479/articles/446619-revisiting-anti-aromaticity-and-chemical-bond-in-planar-bxnx-clusters-x-2-11

Fig. 6. AdNDP bonding pattern for doubly antiaromatic B_2N_2. ON = occupation number

The bonding pattern of B_3N_3 is slightly different, 1c-2e corresponding to N-lone pairs are localized, in agreement with $NICS_{zz}$ isosurface showed previously where local diatropic zones are found. Additionally, 2c-2e corresponding to B-N σ bonds are localized. Finally, three 6c-2e delocalized π bonds are found fulfilling Hückel's rule, which indicates an aromatic compound. This pattern is similar to all remaining aromatic and antiaromatic B_xN_x (x = 3 – 6) clusters (See Fig. S4 – S6 in the SI). The bonding pattern for non-aromatic B_7N_7 cluster presents fourteen 2c-2e σ bonds. The lone pair of nitrogens can no longer be located, so the pattern reveals 14 π bonds in agreement with bond equalization for non-aromatic B_xN_x clusters. This same pattern is observed for clusters with x = 8 – 11 BN moieties (See Fig. S6 – S9 in SI).

Hosted file

image7.emf available at https://authorea.com/users/316479/articles/446619-revisiting-anti-aromaticity-and-chemical-bond-in-planar-bxnx-clusters-x-2-11

Fig. 7. AdNDP bonding pattern for aromatic B_3N_3 and non-aromatic B_7N_7.ON=occupation number

CONCLUSIONS

A complete analysis of the (anti)aromatic character of B_xN_x clusters (x = 2 – 11) has been performed according to magnetic criteria of aromaticity through ring current strength (RCS) analysis, 1D, 2D, 3D $NICS_{zz}$descriptors and AdNDP analysis. The RCS values, FiPC strategy and $NICS_{zz}$-3D-grids patterns show that the B_2N_2 cluster is anti-aromatic. Additionally, the isolines of dissected $NICS_{zz}$ and the bond pattern according to AdNDP reveal that this cluster is doubly anti-aromatic, showing paratropic long-range regions in σ- and π-contributions and delocalized σ- and π-bonds complying with the electron counting rules. For the case of B_3N_3 and B_5N_5 clusters, the $NICS_{zz}$-based strategies show patterns that suggest an aromatic character, in line with this, the AdNDP results show three delocalised 3c-2e bonds and five delocalised 5c-2e bonds for the B_3N_3 and B_5N_5 respectively. For the latter, the $NICS_{zz}$ 3D grids show paratropic contributions in the center of the ring that can be attributed to the contributions of the core electrons of the N and B

atoms, for this reason, isolines of dissected $NICS_{zz}$ were obtained which show that B_5N_5 is non-aromatic σ- and weakly π-aromatic, this is confirmed with RCS values revealing that both clusters are weakly aromatic. The rest of the studied systems (X = 7 – 11) are non-aromatic, FiPC, $NICS_{zz}$ 3D-grids and RCS calculations confirm these results. The AdNDP pattern shows that these clusters have 2X localised σ- and π-bonds which explains the bond length equalisation. Description of aromaticity using $NICS_{zz}$-based descriptors confirms its limitations even though it has good correlations with RCS values, For example, the results of $NICS_{zz}(0)$ present non-negligible positive values for the clusters x = 7 - 11 which could be interpreted as having a certain degree of anti-aromaticity, or the $NICS_{zz}$-scans which present patterns that could lead to incorrect conclusions as mentioned by Cina. Finally, the use of $NICS_{zz}$ descriptor to diagnose (anti)aromaticity must be done carefully. Thus, the use of 1D, 2D or 3D tools based on $NICS_{zz}$ are necessary to have a complete and appropriate description of the aromaticity.

ACKNOWLEDGEMENTS

R.P.-R. thank the financial support of FONDECYT Postdoctorado 3180119, (R.P.-R.). LA thanks Universidad Andres Bello for her PhD scholarship.

REFERENCES

1. Wang, J.; Ma, F.; Sun, M. RSC Advances 2017, 7, 16801-16822.

2. Caldwell, J. D.; Aharonovich, I.; Cassabois, G.; Edgar, J. H.; Gil, B.; Basov, D. N. Nature Reviews Materials 2019, 4, 552-567.

3. Pouch, J. J.; Alterovitz, S. A. Synthesis and properties of boron nitride; Trans Tech, 1990.

4. Khanna, S. N.; Jena, P. Physical Review Letters 1992, 69, 1664-1667.

5. Jena, P.; Sun, Q. Chemical Reviews 2018, 118, 5755-5870.

6. Becker, S.; Dietze, H. J. International Journal of Mass Spectrometry and Ion Processes 1986, 73, 157-166.

7. Seifert, G.; Schwab, B.; Becker, S.; Dietze, H. J. International Journal of Mass Spectrometry and Ion Processes 1988, 85, 327-338.

8. Stéphan, O.; Bando, Y.; Loiseau, A.; Willaime, F.; Shramchenko, N.; Tamiya, T.; Sato, T. Applied Physics A 1998, 67, 107-111.

9. Oku, T.; Nishiwaki, A.; Narita, I. Science and Technology of Advanced Materials 2004, 5, 635-638.

10. Van Orden, A.; Saykally, R. J. Chemical Reviews 1998, 98, 2313-2358.

11. Matxain, J. M.; Ugalde, J. M.; Towler, M. D.; Needs, R. J. The Journal of Physical Chemistry A 2003, 107, 10004-10010.

12. Hückel, E. Zeitschrift für Physik 1931, 70, 204-286.

13. Torres-Vega, J. J.; Vásquez-Espinal, A.; Caballero, J.; Valenzuela, M. L.; Alvarez-Thon, L.; Osorio, E.; Tiznado, W. Inorganic Chemistry 2014, 53, 3579-3585.

14. Fernández, I.; Frenking, G.; Merino, G. Chemical Society Reviews 2015, 44, 6452-6463.

15. Fowler, P. W.; Steiner, E. The Journal of Physical Chemistry A 1997, 101, 1409-1413.

16. Engelberts, J. J.; Havenith, R. W. A.; van Lenthe, J. H.; Jenneskens, L. W.; Fowler, P. W. Inorganic Chemistry 2005, 44, 5266-5272.

17. Kekulé, A. Bulletin mensuel de la Société Chimique de Paris 1865, 3, 98.

18. Martín, N.; Scott, L. T. Chemical Society Reviews 2015, 44, 6397-6400.

19. Krygowski, T. M.; Cyrański, M. K. Chemical Reviews 2001, 101, 1385-1420.

20. Feixas, F.; Matito, E.; Poater, J.; Solà, M. Chemical Society Reviews 2015, 44, 6434-6451.

21. Gershoni-Poranne, R.; Stanger, A. Chemical Society Reviews 2015, 44, 6597-6615.

22. Schleyer, P. v. R.; Maerker, C.; Dransfeld, A.; Jiao, H.; van Eikema Hommes, N. J. R. Journal of the American Chemical Society 1996, 118, 6317-6318.

23. Lazzeretti, P. Physical Chemistry Chemical Physics 2004, 6, 217-223.

24. Pelloni, S.; Monaco, G.; Lazzeretti, P.; Zanasi, R. Physical Chemistry Chemical Physics 2011, 13, 20666-20672.

25. Islas, R.; Martínez-Guajardo, G.; Jiménez-Halla, J. O. C.; Solà, M.; Merino, G. Journal of Chemical Theory and Computation 2010, 6, 1131-1135.

26. Badri, Z.; Pathak, S.; Fliegl, H.; Rashidi-Ranjbar, P.; Bast, R.; Marek, R.; Foroutan-Nejad, C.; Ruud, K. Journal of Chemical Theory and Computation 2013, 9, 4789-4796.

27. Torres-Vega, J. J.; Vásquez-Espinal, A.; Ruiz, L.; Fernández-Herrera, M. A.; Alvarez-Thon, L.; Merino, G.; Tiznado, W. ChemistryOpen 2015, 4, 302-307.

28. Radenković, S.; Bultinck, P. The Journal of Physical Chemistry A 2011, 115, 12493-12502.

29. Carion, R.; Champagne, B.; Monaco, G.; Zanasi, R.; Pelloni, S.; Lazzeretti, P. Journal of Chemical Theory and Computation 2010, 6, 2002-2018.

30. Bultinck, P.; Fias, S.; Ponec, R. Chemistry – A European Journal 2006, 12, 8813-8818.

31. Steiner, E.; Fowler, P. W. Physical Chemistry Chemical Physics 2004, 6, 261-272.

32. Schleyer, P. v. R.; Jiao, H.; Hommes, N. J. R. v. E.; Malkin, V. G.; Malkina, O. L. Journal of the American Chemical Society 1997, 119, 12669-12670.

33. Steiner, E.; Fowler, P. W.; Jenneskens, L. W. Angewandte Chemie International Edition 2001, 40, 362-366.

34. Cernusak, I.; Fowler, P. W.; Steiner, E. Molecular Physics 2000, 98, 945-953.

35. Stanger, A. The Journal of Organic Chemistry 2006, 71, 883-893.

36. Jiménez-Halla, J. O. C.; Matito, E.; Robles, J.; Solà, M. Journal of Organometallic Chemistry 2006, 691, 4359-4366.

37. Merino, G.; Heine, T.; Seifert, G. Chemistry – A European Journal 2004, 10, 4367-4371.

38. Báez-Grez, R.; Ruiz, L.; Pino-Rios, R.; Tiznado, W. RSC Advances 2018, 8, 13446-13453.

39. Báez-Grez, R.; Rabanal-León, W. A.; Alvarez-Thon, L.; Ruiz, L.; Tiznado, W.; Pino-Rios, R. Journal of Physical Organic Chemistry 2018, 0, e3823.

40. Rabanal-León, W. A.; Vásquez-Espinal, A.; Yañez, O.; Pino-Rios, R.; Arratia-Pérez, R.; Alvarez-Thon, L.; Torres-Vega, J. J.; Tiznado, W. European Journal of Inorganic Chemistry 2018, 2018, 3312-3319.

41. Islas, R.; Heine, T.; Merino, G. Accounts of Chemical Research 2012, 45, 215-228.

42. Boldyrev, A. I.; Wang, L.-S. Physical Chemistry Chemical Physics 2016, 18, 11589-11605.

43. Zubarev, D. Y.; Boldyrev, A. I. Physical Chemistry Chemical Physics 2008, 10, 5207-5217.

44. Bader, R. F. W. Atoms in Molecules: A Quantum Theory; Clarendon Press, 1994.

45. Keith, T. A.; Bader, R. F. W. Chemical Physics Letters 1992, 194, 1-8.

46. Keith, T. A.; Bader, R. F. W. The Journal of Chemical Physics 1993, 99, 3669-3682.

47. Keith, T. A.; Bader, R. F. W. Chemical Physics Letters 1993, 210, 223-231.

48. Adamo, C.; Barone, V. The Journal of Chemical Physics 1999, 110, 6158-6170.

49. Weigend, F.; Ahlrichs, R. Physical Chemistry Chemical Physics 2005, 7, 3297-3305.

50. Frisch, M. J.; Trucks, G. W.; Schlegel, H. B.; Scuseria, G. E.; Robb, M. A.; Cheeseman, J. R.; Scalmani, G.; Barone, V.; Mennucci, B.; Petersson, G. A.; Nakatsuji, H.; Caricato, M.; Li, X.; Hratchian, H. P.; Izmaylov, A. F.; Bloino, J.; Zheng, G.; Sonnenberg, J. L.; Hada, M.; Ehara, M.; Toyota, K.; Fukuda, R.; Hasegawa, J.; Ishida, M.; Nakajima, T.; Honda, Y.; Kitao, O.; Nakai, H.; Vreven, T.; Montgomery Jr., J. A.; Peralta, J. E.; Ogliaro, F.; Bearpark, M. J.; Heyd, J.; Brothers, E. N.; Kudin, K. N.; Staroverov, V. N.; Kobayashi, R.; Normand, J.; Raghavachari, K.; Rendell, A. P.; Burant, J. C.; Iyengar, S. S.; Tomasi, J.; Cossi, M.; Rega, N.; Millam, N. J.; Klene, M.; Knox, J. E.; Cross, J. B.; Bakken, V.; Adamo, C.; Jaramillo, J.; Gomperts, R.; Stratmann, R. E.; Yazyev, O.; Austin, A. J.; Cammi, R.; Pomelli, C.; Ochterski, J. W.; Martin, R. L.; Morokuma, K.; Zakrzewski, V. G.; Voth, G. A.; Salvador, P.; Dannenberg, J. J.; Dapprich, S.; Daniels, A. D.; Farkas, Ö.; Foresman, J. B.; Ortiz, J. V.; Cioslowski, J.; Fox, D. J. Gaussian 09 2009.

51. Keith, T. A. AIMAll (Version 190213) Overland Park KS, USA, 2019 (aim.tkgristmill.com).

52. Lu, T.; Chen, F. Journal of Computational Chemistry 2011, 33, 580-592.

53. Jones, L.; Lin, L.; Chamberlain, T. W. Nanoscale 2018, 10, 7639-7648.

54. Bethel, E. W.; Childs, H.; Hansen, C. High Performance Visualization: Enabling Extreme-Scale Scientific Insight; CRC Press, 2012.

55. Rabanal-León, W. A.; Tiznado, W.; Alvarez-Thon, L. International Journal of Quantum Chemistry 2019, 119, e25859.

56. Foroutan-Nejad, C. Theoretical Chemistry Accounts 2015, 134, 8.

57. Islas, R.; Chamorro, E.; Robles, J.; Heine, T.; Santos, J. C.; Merino, G. Structural Chemistry 2007, 18, 833-839.

58. Pino-Rios, R.; Cárdenas-Jirón, G.; Ruiz, L.; Tiznado, W. ChemistryOpen 2019, 8, 321-326.

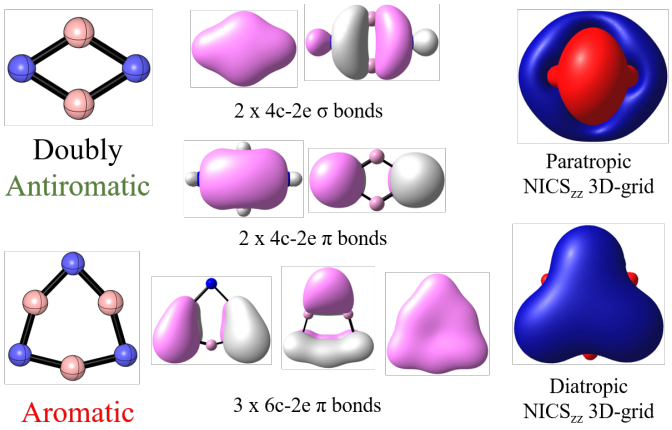

Long-range paratropic and diatropic regions in the center of the ring suggest that B2N2 and B3N3 are antiaromatic and aromatic respectively. AdNDP results reveal that the first is doubly (σ- and π-)antiaromatic and the latter is π-aromatic. The results presented show that the (anti)aromatic character is reduced as the ring expands.